Published in final edited form as:
J Mol Biol. 2010 February 5; 395(5): 908. doi:10.1016/j.jmb.2009.11.029.

A pocket on the surface of the N-terminal BRCT domain of Mcph1 is required to prevent abnormal chromosome condensation

Mark W. Richards[1], **Justin W.C. Leung**[2], **S. Mark Roe**[1], **Junjie Chen**[2], and **Richard Bayliss**[1,*]

[1]Section of Structural Biology, Institute of Cancer Research, Chester Beatty Laboratories, 237 Fulham Road, London, SW3 6JB, UK.

[2]Department of Experimental Radiation Oncology, The University of Texas M. D. Anderson Cancer Center, 1515 Holcombe Boulevard, Houston, Texas 77030, USA.

Abstract

Mcph1 is mutated in autosomal recessive primary microcephaly and premature chromosome condensation (PCC) syndrome. Increased chromosome condensation is a common feature of cells isolated from patients afflicted with either disease. Normal cells depleted of Mcph1 also exhibit a PCC phenotype. Human Mcph1 contains three BRCA1-Carboxyl Terminal (BRCT) domains, the first of which (Mcph1N) is necessary for the prevention of PCC. The only known disease-associated missense mutation in Mcph1 resides in this domain (T27R). We have determined the X-ray crystal structure of human Mcph1N to 1.6Å resolution. Compared with other BRCT domain structures, the most striking differences are an elongated, ordered β1-α1 loop and an adjacent hydrophobic pocket. This pocket is in the equivalent structural position to the phosphate binding site of BRCT domains that recognize phospho-proteins, although the phosphate-binding residues are absent in Mcph1N. Mutations in the pocket abrogate the ability of full-length Mcph1 to rescue the PCC phenotype of Mcph1$^{-/-}$ mouse embryonic fibroblast cells, suggesting that it forms an essential part of a protein-protein interaction site necessary to prevent PCC.

Keywords

Microcephaly; Mcph1; BRCT domain; Premature Chromosome Condensation; X-ray crystallography

The Microcephalin/Mcph1/BRIT1 gene is mutated in autosomal recessive primary microcephaly (MCPH) and premature chromosome condensation (PCC) syndrome [1; 2]. These diseases share characteristic symptoms of below average head diameter, reduced mental capabilities and a cellular phenotype of chromosome condensation in the G2 phase of the cell cycle. Disease-associated mutations in the *Mcph1* gene have been identified that truncate the protein (S25X, 427insA) or that produce a missense mutation (T27R) [1; 3; 4]. Mcph1 expression is reduced in cell lines derived from breast cancers, leading to the suggesting that it may

*Corresponding Author, E-mail address of the corresponding author richard.bayliss@icr.ac.uk.

PDB Accession code
Coordinates and structure factors of Mcph1N have been deposited in the Protein Data Bank (PDB) with accession code 2WT8.

function as a tumour suppressor gene 5. Mcph1 has been linked with DNA damage regulation, repression of gene expression, cell-cycle progression and chromosome condensation, although the precise function of the protein in these processes is not yet clear [5; 6; 7; 8; 9]. Consistent with these functions, Mcph1 normally localises to the centrosome and relocates to sites of DNA repair after cells are exposed to ionizing radiation [5]. Mcph1 contains three BRCA1-Carboxyl Terminal (BRCT) domains: a single domain at the N-terminus and a tandem pair at the C-terminus. BRCT domains function as protein-protein interaction modules, and tandem BRCT domains act as phospho-peptide binding modules [10; 11]. It is reasonable to predict that protein-protein interactions mediated by the BRCT domains of Mcph1 make important contributions to the functions of Mcph1. The interaction of the tandem BRCT domains of Mcph1 with γ-H2AX is crucial for localization to sites of DNA damage after ionizing radiation 12. Mcph1 is recruited early in the DNA repair process, and its depletion disrupts the accumulation of downstream factors. The N-terminal BRCT domain is necessary for prevention of PCC, and contributes to the centrosomal localization of Mcph1, although binding partners for this domain have remained elusive [13; 14].

The structures of several BRCT domains have been reported, including those present in the DNA repair proteins XRCC1 and the tandem domain pair of BRCA1 bound to a phospho-peptide [15; 16; 17]. Despite very low sequence homology, the secondary and tertiary structures of these domains are highly similar, consisting of a central four-stranded parallel β-sheet enclosed by three α-helices [15]. In tandem domains, the phospho-peptide binding site lies at the interface of the two domains, with the residues that recognize the phosphate group on the first domain in the β1-α1 loop and on the N-terminus of α2 [16; 17; 18; 19; 20].

To gain insights into the function of the N-terminal BRCT domain of Mcph1 we determined the X-ray crystal structure of this domain. The domain exhibits a hydrophobic pocket at the equivalent position to the typical phosphate binding site. We show that this pocket is crucial for the rescue of abnormal chromosome condensation in cells lacking wild-type microcephalin.

Human Mcph1 is an 835 amino acid protein that comprises three BRCT domains but no other recognizable domains (Figure 1a). We produced and crystallized a fragment of Mcph1 (Mcph1N) that encompasses the first BRCT domain comprising the first 95 amino acids of Mcph1. Molecular replacement failed with known BRCT domain structures, and as yet no novel individual BRCT domains have been solved using this method. The structure of Mcph1N was solved to 1.6Å by Single wavelength Anomalous Diffraction (SAD) phasing using protein crystals incorporating selenomethionine. The asymmetric unit comprises four copies of Mcph1N two of which extend the full 95 amino acids (chains A and B), and the other two lack the first three amino acids (chains C and D). The refinement and geometry statistics, and the final 2mFo-DFc electron density map are consistent with a high resolution, high quality structure (Table 1, Figure 1b).

DALI was used to identify the most similar BRCT domain structures and to produce the structure-based sequence alignment (Figure 1c 21). The sequence identity between Mcph1N and the other BRCT domains is in the range 9 – 20%, and no residues are identical in all nine proteins. These domains are more highly conserved at the secondary and tertiary structure level (DALI RMSD, root mean square deviation, 1.7 – 3.4 Å). The only structural feature of Mcph1N for which a match was not found among other BRCT domains is the extended loop between β1 and α1, which protrudes an additional ~8Å in Mcph1 when compared to XRCC1 (Figure 1d). This loop is held in an ordered conformation by H-bonds between the mainchain and the sidechains of Ser17 and Asn19 (Figure 1e).

To identify potential surface features that might play a role in the function of this domain, we analyzed the conservation of Mcph1N homologues. Mcph1N is well conserved among

vertebrates and many of the conserved residues are in the four β-strands that are buried in the interior of the protein (Figure 2a). The surfaces of the protein, including the outsides of the four helices, are mostly not conserved, although there is a striking surface patch of conserved residues formed by β1, the β1-α1 loop and α1 (Figure 2b). This patch abuts the site of the microcephaly mutation Thr27, which suggested to us that it might be of functional relevance. We therefore included residues from this region in our functional analysis, as described below.

Inspection of the crystal packing contacts revealed a surface pocket composed of Trp16 and Tyr56 that was involved with two different contacts (Figure 2c). In one type of crystal contact, the sidechain of Lys45 of chain C or chain D packs into the pocket of chain A or chain B respectively. In the other type of crystal contact, the sidechain of Met1 of chain A or chain B packs against the pocket of chain C or chain D respectively. In the first domain of tandem BRCT domains, the equivalent region forms the phosphate-binding pocket in the phospho-peptide binding site, as shown for BRCA1 in the left panel of Figure 2d [19]. In Mcph1N this region is incompatible with phosphate binding because the crucial phosphate-binding residues (i.e. Lys1702, Ser1655 using BRCA1 numbering) are replaced by Thr59 and Glu14 (Figure 2d, centre panel). In addition, the surface of Mcph1N in and around this pocket is acidic rather than basic (Figure 2d, right panel). The tryptophan sidechain is conserved in vertebrates and the tyrosine is less well conserved (Figure 2a), although the substitutions could conserve the hydrophobic nature of the pocket. The fact that this unusual surface feature of Mcph1N occupies the position of the phospho-binding pocket in other BRCT domains suggested to us that it might be involved in protein-protein interactions, and that this site should be included in our functional analysis.

In a population of mouse embryonic fibroblasts (MEFs) prepared from Mcph1$^{-/-}$ knockout mice, approximately 30% of the cells exhibit PCC, which recapitulates the defect observed in cells derived from microcephaly or PCC syndrome patients [14]. The introduction of wild-type Mcph1 in these Mcph1$^{-/-}$ MEFs reduces the proportion of cells that exhibit PCC to 2–3%, which is similar to that observed in wild-type MEFs. 40–50% of the Mcph1$^{-/-}$ MEFs also have abnormally condensed chromosomes during metaphase, which can be rescued by the expression of wild-type Mcph1, but not by a mutant lacking the Mcph1N domain [14]. The Mcph1N domain is therefore crucial for the function of Mcph1 in prevention of abnormal chromosome condensation, and we decided to identify essential residues for this function within Mcph1N. Based on the above structural analysis, we designed several mutations in full-length Mcph1 and tested their abilities to rescue abnormally condensed metaphase chromosomes in Mcph1$^{-/-}$ MEFs. We made Y24A and K53A to disrupt the conserved surface patch (Figure 2b), W16A and Y56S to disrupt the pocket (Figure 2c) and the T27R mutation that was found in a microcephaly patient [4]. The position of these mutations within the Mcph1N structure is shown in Figure 3a. Metaphase spreads were prepared from Mcph1$^{-/-}$ MEFs expressing Mcph1 and the proportion of cells exhibiting abnormally condensed chromosomes were counted (Figure 3b, c). As previously observed, fewer than 10% of wild-type MEFs displayed abnormally condensed chromosomes, whereas almost 50% of the Mcph1−/− MEFs had abnormally condensed chromosomes. Mcph1 containing mutations in the conserved surface patch was able to rescue this metaphase chromosome condensation defect to an extent similar to wild-type Mcph1, ruling out a critical role for this patch in this chromosome condensation function of Mcph1. The T27R mutant of Mcph1 was only slightly impaired in this function, consistent with the previous report that this patient's cells only shows mild PCC phenotype. In contrast, the pocket mutations were significantly reduced in their abilities to rescue this chromosome condensation defect, with almost 30% of cells expressing the W16A mutant of Mcph1 exhibiting abnormally condensed chromosomes. This is very similar to the proportion previously observed with a fragment of Mcph1 lacking the entire Mcph1N domain [14], and therefore the W16A mutation recapitulates the effect of the loss of the domain with respect to chromosome condensation. None of the mutations compromised the ability of Mcph1

to relocate to γ-H2AX foci upon irradiation (Figure 3d), consistent with the previous report that the C-terminal BRCT domains are required for Mcph1 localization to sites of DNA breaks [12]. We used circular dichroism spectroscopy and a thermal shift assay to show that neither pocket mutations nor the T27R microcephaly mutation disrupt the fold of the Mcph1N domain or reduce its thermal stability (Figure 3e,f). Based on these observations, we conclude that the pocket is a crucial feature required for Mcph1 function in the regulation of chromosome condensation.

The phosphate-binding pocket is a conserved feature of the first domain of tandem BRCT repeats and the equivalent site was postulated to be a site of protein-protein interaction on the C-terminal BRCT domain of XRCC1 [15; 16; 17; 18; 19; 20]. We have now shown that the equivalent surface on the N-terminal BRCT domain of Mcph1, on the β1-α1 loop and the N-terminus of α2, is a functionally important site for Mcph1 function in prevention of abnormal metaphase chromosome condensation. This region of the BRCT domain is the most divergent structurally from other BRCT domains, due to the more elongated β1-α1 loop and the presence of a pair of surface aromatic sidechains. This pocket is presumably a crucial element of the interface of a protein-protein interaction. Future work will identify the binding partners of Mcph1 that mediate its function in prevention of PCC, and define the structural basis of their interactions.

Acknowledgments

RB acknowledges the support of a Royal Society University Research Fellowship, Cancer Research UK (C24461/A8032, C24461/A9549), the Medical Research Council (G0800021), the Career Development Faculty Programme of The Institute of Cancer Research, infrastructural support from Cancer Research UK for Structural Biology at ICR and NHS funding to the NIHR Biomedical Research Centre. JC was supported by grants from the National Institutes of Health. JC is also a recipient of an Era of Hope Scholar award from the Department of Defense and a member of the Mayo Clinic Breast SPORE program. We are indebted to the staff of DIAMOND beamline I03 for their support during data collection and to the ISMB Biophysics Centre at Birkbeck, University of London, UK for use of their circular dichroism instrument.

References

1. Trimborn M, Bell SM, Felix C, Rashid Y, Jafri H, Griffiths PD, Neumann LM, Krebs A, Reis A, Sperling K, Neitzel H, Jackson AP. Mutations in microcephalin cause aberrant regulation of chromosome condensation. Am J Hum Genet 2004;75:261–266. [PubMed: 15199523]
2. Woods CG, Bond J, Enard W. Autosomal recessive primary microcephaly (MCPH): a review of clinical, molecular, and evolutionary findings. Am J Hum Genet 2005;76:717–728. [PubMed: 15806441]
3. Jackson AP, Eastwood H, Bell SM, Adu J, Toomes C, Carr IM, Roberts E, Hampshire DJ, Crow YJ, Mighell AJ, Karbani G, Jafri H, Rashid Y, Mueller RF, Markham AF, Woods CG. Identification of microcephalin, a protein implicated in determining the size of the human brain. Am J Hum Genet 2002;71:136–142. [PubMed: 12046007]
4. Trimborn M, Richter R, Sternberg N, Gavvovidis I, Schindler D, Jackson AP, Prott EC, Sperling K, Gillessen-Kaesbach G, Neitzel H. The first missense alteration in the MCPH1 gene causes autosomal recessive microcephaly with an extremely mild cellular and clinical phenotype. Hum Mutat 2005;26:496. [PubMed: 16211557]
5. Rai R, Dai H, Multani AS, Li K, Chin K, Gray J, Lahad JP, Liang J, Mills GB, Meric-Bernstam F, Lin SY. BRIT1 regulates early DNA damage response, chromosomal integrity, and cancer. Cancer Cell 2006;10:145–157. [PubMed: 16872911]
6. Lin SY, Elledge SJ. Multiple tumor suppressor pathways negatively regulate telomerase. Cell 2003;113:881–889. [PubMed: 12837246]
7. Xu X, Lee J, Stern DF. Microcephalin is a DNA damage response protein involved in regulation of CHK1 and BRCA1. J Biol Chem 2004;279:34091–34094. [PubMed: 15220350]

8. Lin SY, Rai R, Li K, Xu ZX, Elledge SJ. BRIT1/MCPH1 is a DNA damage responsive protein that regulates the Brca1-Chk1 pathway, implicating checkpoint dysfunction in microcephaly. Proc Natl Acad Sci U S A 2005;102:15105–15109. [PubMed: 16217032]
9. Alderton GK, Galbiati L, Griffith E, Surinya KH, Neitzel H, Jackson AP, Jeggo PA, O'Driscoll M. Regulation of mitotic entry by microcephalin and its overlap with ATR signalling. Nat Cell Biol 2006;8:725–733. [PubMed: 16783362]
10. Yu X, Chini CC, He M, Mer G, Chen J. The BRCT domain is a phospho-protein binding domain. Science 2003;302:639–642. [PubMed: 14576433]
11. Manke IA, Lowery DM, Nguyen A, Yaffe MB. BRCT repeats as phosphopeptide-binding modules involved in protein targeting. Science 2003;302:636–639. [PubMed: 14576432]
12. Wood JL, Singh N, Mer G, Chen J. MCPH1 functions in an H2AX-dependent but MDC1-independent pathway in response to DNA damage. J Biol Chem 2007;282:35416–35423. [PubMed: 17925396]
13. Jeffers LJ, Coull BJ, Stack SJ, Morrison CG. Distinct BRCT domains in Mcph1/Brit1 mediate ionizing radiation-induced focus formation and centrosomal localization. Oncogene 2008;27:139–144. [PubMed: 17599047]
14. Wood JL, Liang Y, Li K, Chen J. Microcephalin/MCPH1 associates with the Condensin II complex to function in homologous recombination repair. J Biol Chem 2008;283:29586–29592. [PubMed: 18718915]
15. Zhang X, Morera S, Bates PA, Whitehead PC, Coffer AI, Hainbucher K, Nash RA, Sternberg MJ, Lindahl T, Freemont PS. Structure of an XRCC1 BRCT domain: a new protein-protein interaction module. EMBO J 1998;17:6404–6411. [PubMed: 9799248]
16. Clapperton JA, Manke IA, Lowery DM, Ho T, Haire LF, Yaffe MB, Smerdon SJ. Structure and mechanism of BRCA1 BRCT domain recognition of phosphorylated BACH1 with implications for cancer. Nat Struct Mol Biol 2004;11:512–518. [PubMed: 15133502]
17. Shiozaki EN, Gu L, Yan N, Shi Y. Structure of the BRCT repeats of BRCA1 bound to a BACH1 phosphopeptide: implications for signaling. Mol Cell 2004;14:405–412. [PubMed: 15125843]
18. Williams RS, Lee MS, Hau DD, Glover JN. Structural basis of phosphopeptide recognition by the BRCT domain of BRCA1. Nat Struct Mol Biol 2004;11:519–525. [PubMed: 15133503]
19. Stucki M, Clapperton JA, Mohammad D, Yaffe MB, Smerdon SJ, Jackson SP. MDC1 directly binds phosphorylated histone H2AX to regulate cellular responses to DNA double-strand breaks. Cell 2005;123:1213–1226. [PubMed: 16377563]
20. Kilkenny ML, Dore AS, Roe SM, Nestoras K, Ho JC, Watts FZ, Pearl LH. Structural and functional analysis of the Crb2-BRCT2 domain reveals distinct roles in checkpoint signaling and DNA damage repair. Genes Dev 2008;22:2034–2047. [PubMed: 18676809]
21. Holm L, Sander C. Protein structure comparison by alignment of distance matrices. J Mol Biol 1993;233:123–138. [PubMed: 8377180]
22. CCP4. The CCP4 (Collaborative Computational Project Number 4) suite: programmes for protein crystallography. Acta Crystallogr D Biol Crystallogr 1994;50:760–763. [PubMed: 15299374]
23. Adams PD, Grosse-Kunstleve RW, Hung LW, Ioerger TR, McCoy AJ, Moriarty NW, Read RJ, Sacchettini JC, Sauter NK, Terwilliger TC. PHENIX: building new software for automated crystallographic structure determination. Acta Crystallogr D Biol Crystallogr 2002;58:1948–1954. [PubMed: 12393927]
24. Emsley P, Cowtan K. Coot: model-building tools for molecular graphics. Acta Crystallogr D Biol Crystallogr 2004;60:2126–2132. [PubMed: 15572765]
25. DeLano WL. The PyMOL Molecular Graphics System. 2002
26. Ghosh A, Shuman S, Lima CD. The structure of Fcp1, an essential RNA polymerase II CTD phosphatase. Mol Cell 2008;32:478–490. [PubMed: 19026779]
27. Derbyshire DJ, Basu BP, Serpell LC, Joo WS, Date T, Iwabuchi K, Doherty AJ. Crystal structure of human 53BP1 BRCT domains bound to p53 tumour suppressor. EMBO J 2002;21:3863–3872. [PubMed: 12110597]
28. Joo WS, Jeffrey PD, Cantor SB, Finnin MS, Livingston DM, Pavletich NP. Structure of the 53BP1 BRCT region bound to p53 and its comparison to the Brca1 BRCT structure. Genes 2002;16:583–593.

29. Lee MS, Edwards RA, Thede GL, Glover JN. Structure of the BRCT repeat domain of MDC1 and its specificity for the free COOH-terminal end of the gamma-H2AX histone tail. J Biol Chem 2005;280:32053–32056. [PubMed: 16049003]

30. Williams RS, Green R, Glover JN. Crystal structure of the BRCT repeat region from the breast cancer-associated protein BRCA1. Nat Struct Biol 2001;8:838–842. [PubMed: 11573086]

31. Larkin MA, Blackshields G, Brown NP, Chenna R, McGettigan PA, McWilliam H, Valentin F, Wallace IM, Wilm A, Lopez R, Thompson JD, Gibson TJ, Higgins DG. Clustal W and Clustal X version 2.0. Bioinformatics 2007;23:2947–2948. [PubMed: 17846036]

32. Lees JG, Smith BR, Wien F, Miles AJ, Wallace BA. CDtool-an integrated software package for circular dichroism spectroscopic data processing, analysis, and archiving. Anal Biochem 2004;332:285–289. [PubMed: 15325297]

33. Niesen FH, Berglund H, Vedadi M. The use of differential scanning fluorimetry to detect ligand interactions that promote protein stability. Nat Protoc 2007;2:2212–2221. [PubMed: 17853878]

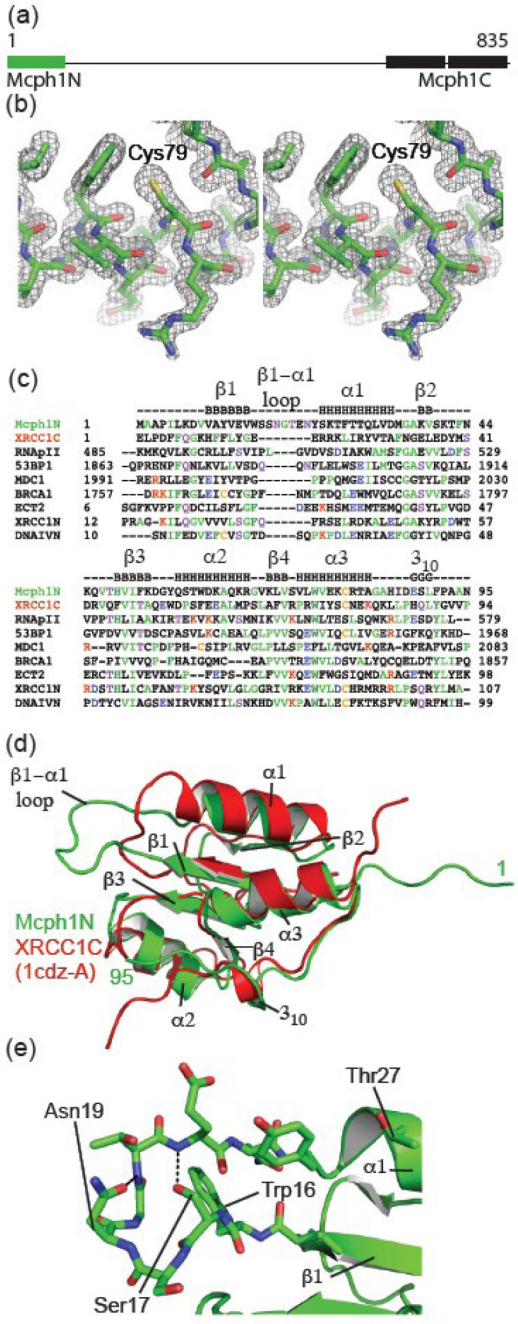

Figure 1. X-ray crystal structure of the first BRCT domain of Mcph1

(a) The domain structure of Mcph1. The N-terminal BRCT domain (Mcph1N) is shown as a green box, the C-terminal tandem BRCT domains (Mcph1C) are shown as black boxes. (b) A stereo diagram showing a representative region of the refined structure and 2mFo-DFc electron density contoured at 1.0σ. All structure figures were made using PyMOL 25. (c) The secondary structure assignment of Mcph1N is shown above a structure-based sequence alignment of its closest structural homologues. Abbreviated names of structural homologues are shown on the left: XRCC1C - XRCC1 C-terminal domain (1cdz chain A15); RNApII - RNA polymerase II (3ef1 chain A26); 53BP1 - 53BP1 second domain of tandem (1gzh chain D27, 1kzy chain D28) ; MDC1 – MDC1 second domain of tandem (2ado chain A29, 2azm chain A 19); BRCA1

- BRCA1 second domain of tandem (1jnx chain X 30) ; ECT2 - ECT2 C-terminal domain (2cou); XRCC1N - XRCC1 N-terminal domain (2d8m); DNAIVN - DNA ligase IV N-terminal domain (2e2w), The residue numbering is taken from the coordinate files. (d) A cartoon representation of the superposition of Mcph1N (green) with XRCC1C (red). The secondary structure elements and the first and last residues of Mcph1N are labeled. (e) A magnified view of the β1-α1 loop region of Mcph1N. The putative H-bonds between sidechain residues and the mainchain are shown as dashed lines.

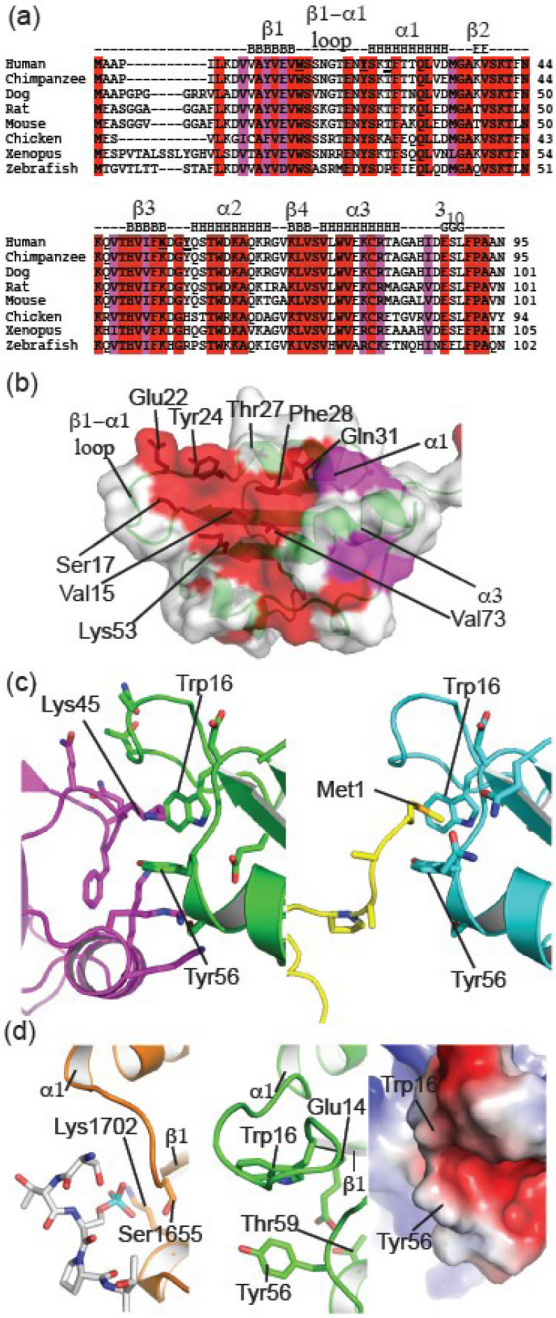

Figure 2. Identification of potential functional sites on the surface of Mcph1N

(a) The sequence conservation among vertebrate Mcph1 homologues is shown using the color scheme: red for identical; magenta for conserved, grouped by (ILVM), (YF), (DE), (RK), (ST); white for non-conserved. The sequence alignment was made using ClustalW 31. (b) Sequence conservation as defined in (a) mapped onto the surface of Mcph1N. The microcephaly mutation T27R and residues that form a conserved surface patch are marked. (c) The two different crystal contacts that involve the surface pocket formed by Trp16 and Tyr56 are shown using a cartoon representation of the protein mainchain and a stick representation of the interacting sidechains. The colour scheme used is: chain A green, chain B yellow, chain C magenta, chain D cyan. (d) The left panel shows the binding of phospho-peptide (grey carbon atoms) to the first domain

of BRCA1 BRCT tandem pair (orange cartoon and carbon atoms) 19. The central panel shows the equivalent region of Mcph1N in the same view. The right panel shows the electrostatic potential (colour ramped from red=negative to blue=positive, calculated using PyMOL) of the Mcph1N surface in a view rotated by ~90°.

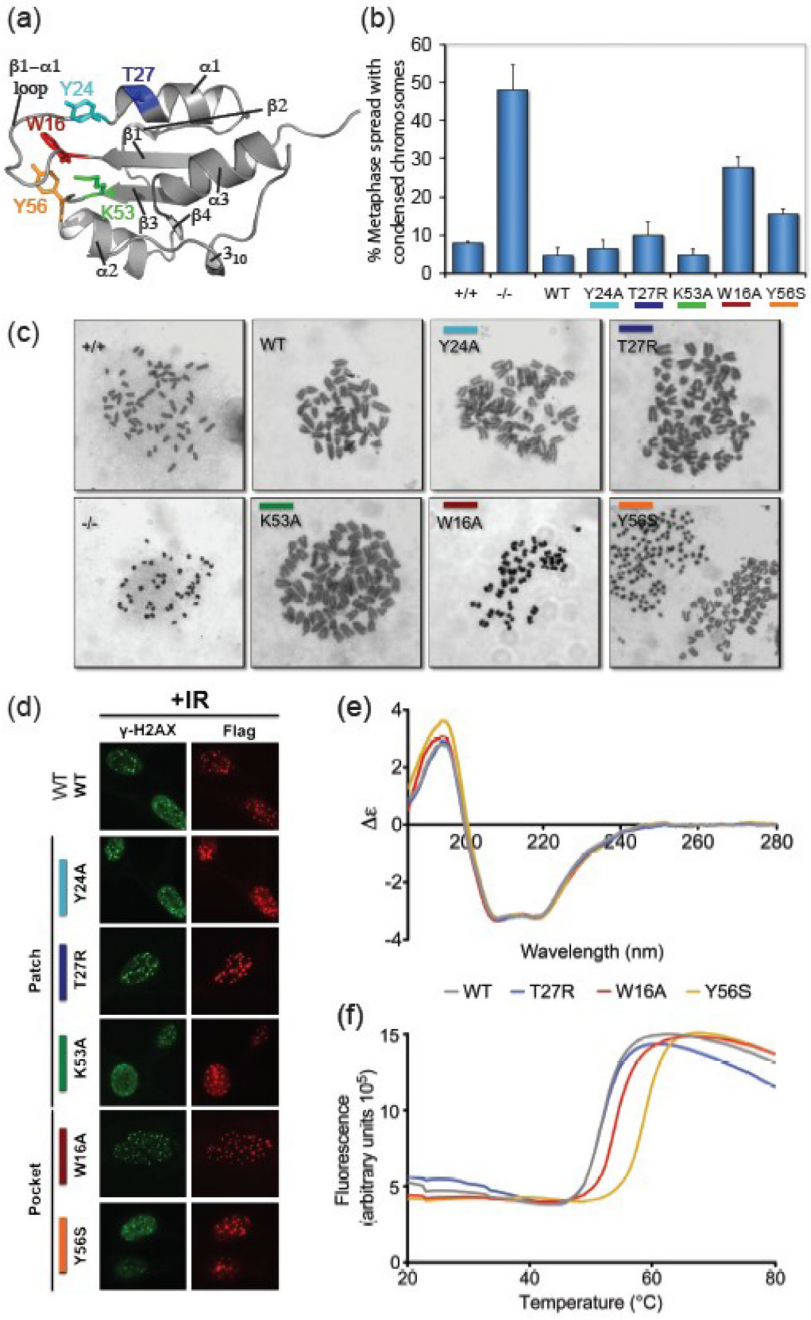

Figure 3. Pocket mutations do not rescue the abnormal chromosome condensation phenotype of Mcph1$^{-/-}$ cells

(a) The position of residues mutated in this study on the structure of Mcph1N. (b,c) Rescue of premature chromosome condensation (PCC) phenotype of Mcph1$^{-/-}$ MEFs by wild-type (WT) or mutant Mcph1. (b) Shows the quantification of metaphase cells with condensed chromosomes observed in each indicated cell line. (c) Shows examples of metaphase spreads seen in these cell lines. (d) Proper localisation of wild-type and mutant Mcph1 to γ-H2AX foci upon ionizing radiation (IR). Cell culture, transfection, chromosome spreads, irradiation and immunofluorescence were carried out as described in 14. (e) Circular dichroism spectroscopy shows that the WT, T27R, W16A and Y56S Mcph1N domain proteins are folded. Spectra were

collected using 1 mg/ml samples in 10mM sodium phosphate pH 7.5, 20 mM sodium chloride in a 0.01 cm pathlength quartz cell at 18 °C on an Aviv 202SF instrument (Aviv Biomedical). Data were processed using CDTool software 32. (f) A thermal shift assay shows that the T27R, W16A and Y56S Mcph1N domain proteins are at least as thermally stable as the WT domain protein. The thermal shift assay is based on the increased fluorescence of a dye upon binding to the exposed hydrophobic core of proteins unfolded by a temperature gradient 33. 25 ml samples containing 0.3 mg/ml protein and 5x Sypro Orange dye (Sigma) in 10 mM sodium phosphate pH 7.5, 20 mM sodium chloride were heated from 4–95 °C at 2 °C/min in a BioRad IQ5 instrument and monitored at excitation and emission wavelengths of 485 nm and 585 nm. The mean of eight denaturation curves was calculated for each protein and the buffer alone; the baseline was then subtracted. Data were fitted to a Boltzmann sigmoid function to yield temperatures of 50% denaturation (apparent T_m) of 52.6 °C (WT), 52.7 °C (T27R), 55.1°C (W16A), 59.5 °C (Y56S).

Table 1

Summary of crystallographic analysis

His_6-tagged Mcph1N protein was expressed in B834 cells co-transformed with the CodonPlus RIL plasmid grown in SelenoMet Medium (Molecular Dimensions). The protein was purified using a 5ml chelating Sepharose column (GE Healthcare) that had been charged with nickel and equilibrated with 100 mM sodium phosphate pH 7.5, 0.5 M NaCl. The column was washed with 50 mM imidazole and eluted on a gradient 50–500 mM imidazole in this buffer. The eluted protein was cleaved using His-tagged TEV protease for 3 hours at 21°C. The cleaved protein was passed through a second nickel column to remove the tag and protease. The protein was dialysed into 20 mM sodium phosphate pH 6.0, 1 mM EDTA, 50 mM sodium chloride and applied to a SP Sepharose column (GE Healthcare). The protein was eluted on a gradient 50–750 mM sodium chloride in this buffer. The eluted protein was further purified by gel filtration on a Superdex 75 16/60 column equilibrated in 20 mM Tris-HCl pH 7.5, 80 mM NaCl. Crystals were grown at 18 °C using the hanging-drop vapour diffusion method using 100 mM MES pH 6.0, 18% PEG 6000, 200 mM ammonium chloride in the reservoir. 2 µl of 15 mg/ml protein stock was mixed with 2 µl of reservoir solution to form the drop and then microseeded. Crystals were flash-frozen in reservoir solution supplemented with 20% glycerol. X-ray diffraction data was processed using CCP4 software [22]. The structure of Mcph1N was solved using Phenix 23 to locate the selenium sites, automatically build the four protein chains and for refinement. Manual rebuilding was carried out using Coot 24.

Crystals		
Spacegroup		$P2_1$
Lattice constants	*a* (Å)	80.98
	b (Å)	34.21
	c (Å)	84.24
	β (°)	113.53
Data collection		
X-ray source		Diamond I03
Wavelength (Å)		0.92
Resolution range (Å)		45.3-1.6
(Highest resolution shell)		(1.69-1.60)
Unique reflections		56453 (8180)
Completeness(%)		99.7 (99.9)
Multiplicity		4.3 (3.6)
Rmerge (%)		5.2 (33.6)
I/σ(I)		16.1 (3.2)
Refinement		
Resolution range (Å)		45.3-1.6
Number of:	amino acids	377
	waters	469
*R*factor (%)		19.02
*R*free[a] (%)		22.21
Bond deviation (Å)		0.007
Angle deviation (°)		1.057
Molprobity output scores		
All-atom Clashscore		8.15
Bad rotamers (%)		2.5

Ramachandran outliers (%)	0.0
Ramachandran favoured (%)	98.6

[a] Free *R*factor was computed using 5% of the data assigned randomly [30].